学位論文

In vivo Electron Paramagnetic Resonance Tooth Dosimetry: Dependence of Radiation-induced Signal Amplitude on the Enamel Thickness and Surface Area of *ex vivo* Human Teeth

香川大学大学院医学系研究科
分子情報制御医学専攻

馬越　通崇

Paper

IN VIVO ELECTRON PARAMAGNETIC RESONANCE TOOTH DOSIMETRY: DEPENDENCE OF RADIATION-INDUCED SIGNAL AMPLITUDE ON THE ENAMEL THICKNESS AND SURFACE AREA OF EX VIVO HUMAN TEETH

Michitaka Umakoshi,* Ichiro Yamaguchi,† Hiroshi Hirata,‡ Naoki Kunugita,† Benjamin B. Williams,§ Harold M. Swartz,§ and Minoru Miyake*

Abstract—**In vivo L-band electron paramagnetic resonance tooth dosimetry is a newly developed and very promising method for retrospective biodosimetry in individuals who may have been exposed to significant levels of ionizing radiation. The present study aimed to determine the relationships among enamel thickness, enamel area, and measured electron paramagnetic resonance signal amplitude with a view to improve the quantitative accuracy of the dosimetry technique. Ten isolated incisors were irradiated using well-characterized doses, and their radiation-induced electron paramagnetic resonance signals were measured. Following the measurements, the enamel thickness and area of each tooth were measured using micro-focus computed tomography. Linear regression showed that the enamel area at each measurement position significantly affected the radiation-induced electron paramagnetic resonance signal amplitude ($p < 0.001$). Simulation data agreed well with this result. These results indicate that it is essential to properly consider enamel thickness and area when interpreting electron paramagnetic resonance tooth dosimetry measurements to optimize the accuracy of dose estimation.**

Health Phys. 113(4):262–270; 2017

Key words: computed tomography; dose assessment; dosimetry; radiation, ionizing

*Department of Oral and Maxillofacial Surgery, Faculty of Medicine, Kagawa University, Kagawa,761-0793, Japan; †Department of Environmental Health, National Institute of Public Health, Wako, 351-0197, Japan; ‡Division of Bioengineering and Bioinformatics, Graduate School of Information Science and Technology, Hokkaido University, Sapporo, 060-0814, Japan; §EPR Center for the Study of Viable Systems, Department of Radiology, The Geisel School of Medicine at Dartmouth, Lebanon, NH 03766.

The authors declare no conflicts of interest.

For correspondence contact: Minoru Miyake, 1750-1 Ikenobe, Miki-cho, Kita-gun, Kagawa, 761-0793, Japan, or email at dentmm@med.kagawa-u.ac.jp.

(*Manuscript accepted* 26 *April* 2017)
0017-9078/17/0

DOI: 10.1097/HP.0000000000000698

INTRODUCTION

IN THE CONTEXT of a nuclear event, with the potential for exposure of a large number of people to life-threatening doses of ionizing radiation, the availability and use of effective biodosimetry methods could play a crucial role in the management of radiation injuries. In vivo electron paramagnetic resonance (EPR) tooth dosimetry has a number of unique characteristics and capabilities that may help with triage.

EPR spectroscopy is a well-established physical retrospective biodosimetry method that has applications related to unplanned exposure to radiation (Ikeya et al. 1984, 1986). The technique exploits the fact that radicals generated by ionizing radiation are extremely stable within the matrix of the bone and teeth. Specifically, radicals created in the tooth enamel remain for thousands of years and are generated in direct proportion to the applied dose of photon and charged particle radiation (Desrosiers and Schauer 2001). EPR tooth dosimetry for extracted teeth has been used widely for many years. Conventionally, EPR tooth dosimetry has been performed in isolated teeth within the X band (approximately 9 GHz), where high detection sensitivity enables estimation of the absorbed dose with very high precision. The disadvantage of X-band methods is that they require enamel tissue sampling as opposed to direct non-invasive measurement, and this may preclude the examination of a large number of people with these methods.

The development of EPR spectrometers using methods that rely on lower microwave frequencies (1.2 GHz, termed as L-band) for in vivo EPR tooth dosimetry has made it possible to measure intact teeth in vivo, thereby enabling the non-invasive estimation of absorbed doses in individual subjects (Miyake et al. 2000). Such lower frequency-based EPR spectrometers could be used to help overcome the challenges associated with managing potential irradiation of thousands of individuals over a short period by allowing on-site determination of whether a particular individual needs to be entered into the medical system for decisions

on treatment initiation and/or mitigation (Swartz et al. 2010, 2012; Williams et al. 2010, 2011a and b, 2014; Flood et al. 2011, 2014).

This in vivo method makes rapid and accurate measurements possible even outside of a traditional laboratory by using the two central maxillary incisors for measurement purposes (Williams et al. 2014). Previously, molars were measured using a resonator, which attached at the top of the tooth to cover the biting surface of these teeth because these measurements were considered the most reliable. However, because of the high incidence of dental restorations in these teeth and the difficulty of rapidly and easily accessing them, measurements are now performed at the incisors using a surface-type resonator (Swartz et al. 2005; Williams et al. 2010). The ease of access to the incisors is an additional potential advantage, especially when considering that measurements in the field are likely to be made by very minimally trained individuals (Williams et al. 2010). Unlike the incisors, the molars are highly unlikely to reflect potentially confusing radiation-induced signals (RIS) triggered by ultraviolet light (UV). The incisors have a smoother surface, facilitating accurate and reproducible placement of the resonator loop.

The decision to perform measurements in the incisors necessitated the design and fabrication of new resonators with smaller detection loops, as the use of larger resonators intended for molars leads to suboptimal EPR detection sensitivity owing to the poor filling factor and heterogeneity of the B1 field distribution (Pollock et al. 2010; Sugawara et al. 2014). Small resonator detection loops can be placed at different locations on the anterior surface of the central maxillary incisors.

A previous study has shown that the strength of RIS is dependent on where the detection loop is placed on the tooth (Pollock et al. 2010), probably because the overall volume that is sampled changes with the placement of the loop at different locations, which then affects the intensity of the RIS.

The present study aimed to determine the relationships among enamel thickness, enamel area, and RIS amplitude and identify the most appropriate locations for placement of the detection loop on the tooth surface. The findings will help optimize the effectiveness of the measurement of the radiation dose using electron paramagnetic resonance biodosimetry based on RIS in incisors.

MATERIALS AND METHODS

Radiation dose measurements in irradiated teeth

The study protocol was approved by the Internal Review Boards of the National Institute of Public Health (NIPH), Japan (approval number: NIPH-IBRA#10039) and Kagawa University (approval number: Heisei#24-4). The authors used 10 extracted complete, intact maxillary central human incisors donated by Japanese subjects. The selected teeth had no significant dental cavities or metal fillings. Before irradiation, the teeth were measured individually using a 1.2 GHz L-band EPR spectrometer (Swartz et al. 2014) at the National Institute of Public Health in Japan to record the background signal amplitude. Each tooth was then serially irradiated with x rays to accumulated doses of 1, 5, 10, and 20 Gy and was re-measured after each dose. Irradiation was performed using a Hitachi Medical x-ray apparatus (MBR-1505R2; Hitachi Medical, Tokyo) at 150 kV and 4 mA, with 0.1 mm copper + 0.3 mm aluminum filtering. The air kerma generated by the x-ray equipment was continuously monitored in an air chamber (N31003; Toyo Medic, Tokyo, Japan). The air chamber was calibrated at the Japan Quality Assurance Organization using a secondary standard dosimeter (Exradin A3 Ion Chamber; Standard Imaging Inc., Middleton, WI, USA) that was certified by the Japan Calibration Service System. The expanded standard uncertainty of the air chamber (coverage factor k = 2) was 5%. EPR spectra were measured using a 1.2 GHz clinical L-band EPR spectrometer. The surface coil (a circular loop with a mean diameter of 7 mm) was formed using 1.0-mm-thick silver wire. Details of the surface loop have been reported elsewhere (Sugawara et al. 2014).

Each tooth was positioned precisely using a custom-made bite block that positioned each tooth within the central homogeneous region of the magnet. Each tooth sample was placed in a dental putty mold (EXAFINE [putty type]; GC Corporation, Tokyo, Japan) to ease both handling and positioning within the bite block (Fig. 1). It was confirmed that the dental putty did not contribute significantly to the EPR signals.

For each tooth and at each dose, measurements were obtained with the detection loop placed at the following three different positions over the tooth surface: center of

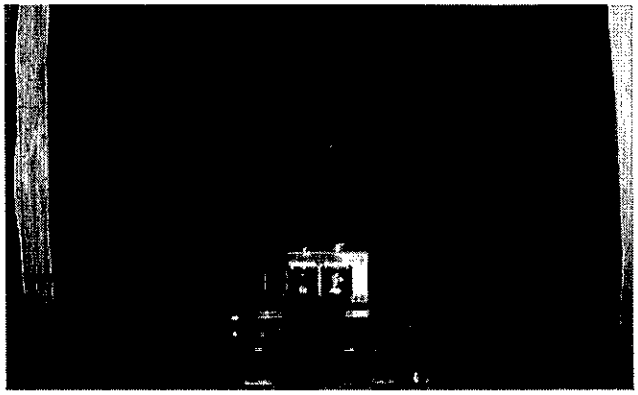

Fig. 1. The surface coil resonator used for measuring sample teeth (a circular loop and a mean diameter of 7 mm). Each tooth sample was placed in a dental putty mold to ease both handling and positioning within the bite block.

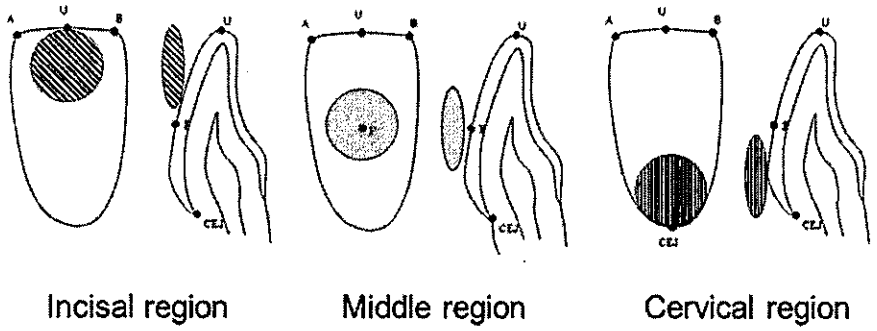

Fig. 2. Schematic showing the measurement position of the detection loop over the surface of the maxillary central incisor tooth.

the cervical region (near the gingival line), middle region of the tooth, and incisal region of the tooth (Fig. 2). The measurement points are shown in Fig. 3. The loop was placed so that the radio frequency (RF) magnetic field generated at the center of the detection loop was perpendicular to the static magnetic field, and the plane of the loop was parallel to the surface of the tooth. The loop placement locations were consistent across all teeth. The EPR spectra were acquired using standard parameters (scan range, 2.5 mT; scan time, 3 s; average scans, 30; modulation amplitude, 0.4 mT) (Miyake et al. 2000; Iwasaki et al. 2005). This process was repeated for a total of five data sets for each dose, as well as before experimental irradiation. A plastic tube containing a solution of 4-oxo-2,2,6,6,-tetramethylpiperidine-d16-1-^{15}N-1-oxyl (^{15}N-PDT, also known as perdeuterated tempone) was placed in close proximity to the surface loop and was used as a reference standard, as well as to monitor EPR signal detection and the amplitude of magnetic field modulation (Williams et al. 2011a). The position of the plastic tube was adjusted to ensure that the EPR signals from ^{15}N-PDT were comparable to RIS at an average dose level.

The ^{15}N-PDT EPR spectrum includes two resonance peaks that are offset from the peak of the irradiated tooth. The ^{15}N-PDT signal has many quality control purposes, including continuous overall verification that the spectrometer is operating correctly, accurate measurement of the amplitude of the applied modulation field, calibration of the magnetic field scan width, and absolute physical magnetic field calibration for each of the recorded spectra for use in data analysis (Williams et al. 2011a). The spectra from each of the collected data sets were analyzed using nonlinear least-squares fitting to estimate the peak-to-peak signal amplitudes of the radiation-induced signals and of ^{15}N-PDT (Fig. 4). These were then averaged to obtain the mean amplitude for each tooth at each dose (VRIS and VPDT, respectively). To account for variations in the RIS amplitude that result from instrumental variability or external environmental factors, the ratio of VRIS to VPDT for each measurement was calculated and normalized to the same ratio for a standard tooth irradiated to 20 Gy. Accordingly, the dosimetric relative RIS amplitude value (RelRIS) associated with each tooth was calculated using the following equation:

$$RelRIS = \left(\frac{V_{RIS}}{V_{PDT}}\right) \Big/ \left(\frac{V_{RIS,20Gy}}{V_{PDT,20Gy}}\right). \quad (1)$$

For each data set, this dosimetric value was related to an estimated absorbed dose using an empirically based calibration.

Enamel thickness and enamel area of the maxillary incisor at each measurement position

After the EPR spectra were recorded, the labial enamel thickness and enamel area at each measurement position were estimated using x-ray micro-focus computed tomography (CT) measurements (inspeXio SMX-90CT; Shimadzu,

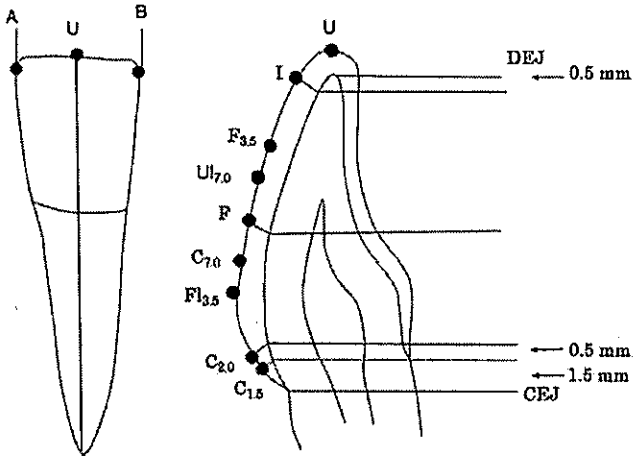

Fig. 3. Measurment points. Left-hand schematic: The tooth was sectioned parallel to the mid-point (point U) between point A and point B. Right-hand schematic: The enamel measurement points over the labial surface (sagittal plane at point U). CEJ—cement enamel junction; DEJ—dentin enamel junction Point I: 0.5 mm toward the gingiva from the dentin-enamel junction (DEJ); point F: the mid-point between the DEJ and cement-enamel junction (CEJ); point C2.0: 2.0 mm toward the incisal edge from the CEJ; point C1.5: 1.5 mm toward the incisal edge from the CEJ; point U: the incisal edge; point UI7.0: 7.0 mm toward the gingiva from point U; point F3.5: 3.5 mm toward the incisal edge from point F; point FI3.5: 3.5 mm toward the gingiva from point F; and point C: 7.0-7.0 mm toward the incisal edge from the CEJ.

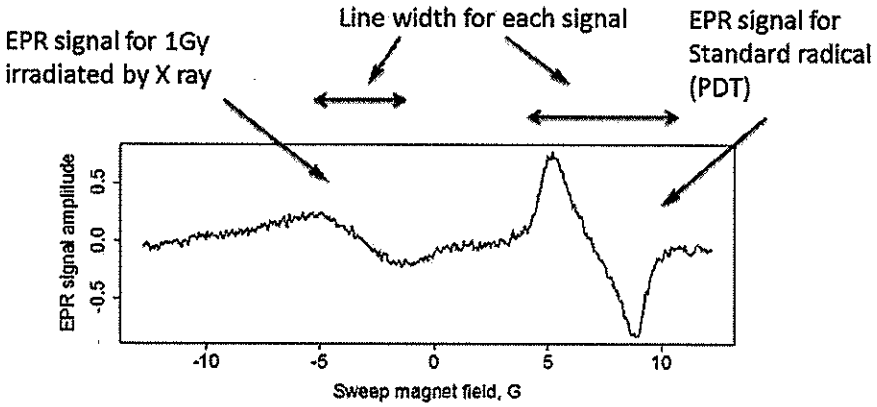

Fig. 4. EPR spectra (observed signal and fitting signal) from an extracted tooth that had been irradiated at 1 Gy. The RIS g-factors are consistent with 2.009, and the PDT g-factors are consistent with 2.007. The x-axis is the magnetic field. The y-axis is the EPR signal amplitude.

Kyoto, Japan). Micro-focus CT was performed after EPR to avoid any confounding influence of the ionizing radiation from the CT. The micro-focus CT imaging parameters were as follows: source to image receptor distance (SID) = 300.0 mm, source to object distance (SOD) = 108.1 mm, and voxel size = 0.055 mm pixel^{-1}.

Measurements of enamel thickness were made using Chen's method with five additional measurement points (Chen et al. 2003). The labial enamel thickness and enamel area were estimated using Osirix™ imaging software (Ver. 5.8.5 on MacOS.10.9; Fig. 3) at the following four points: (1) point I, 0.5 mm toward the gingiva from the dentin-enamel junction (DEJ); (2) point F, the mid-point between the DEJ and cement-enamel junction (CEJ); (3) point C2.0, 2.0 mm toward the incisal edge from the CEJ; and (4) point C1.5, 1.5 mm toward the incisal edge from the CEJ. Five additional measurement points were specified to define the enamel area within the central sagittal plane, as denoted in Fig. 3: (1) point U, the incisal edge; (2) point Ul7.0, 7.0 mm toward the gingiva from point U; (3) point F3.5, 3.5 mm toward the incisal edge from point F; (4) point Fl3.5, 3.5 mm toward the gingiva from point F; and (5) point C, 7.0-7.0 mm toward the incisal edge from the CEJ. The labial enamel area was measured as shown in Fig. 5.

Simulation of magnetic energy stored in the enamel

The EPR signal intensity (S) is proportional to the product of the quality factor (Q) of the resonator with the sample present and the filling factor μ of the resonator. It can be expressed as follows:

$$S \propto x\eta Q\sqrt{P_{in}}, \qquad (2)$$

where "x" is the magnetic susceptibility of the sample, and P_{in} is the incident microwave power (Feher 1957). The filling factor μ (eqn 2) is equal to the ratio of the magnetic energy of the radio frequency (RF) in the sample to the total RF magnetic energy in the resonator system. Electromagnetic fields around the surface coil were

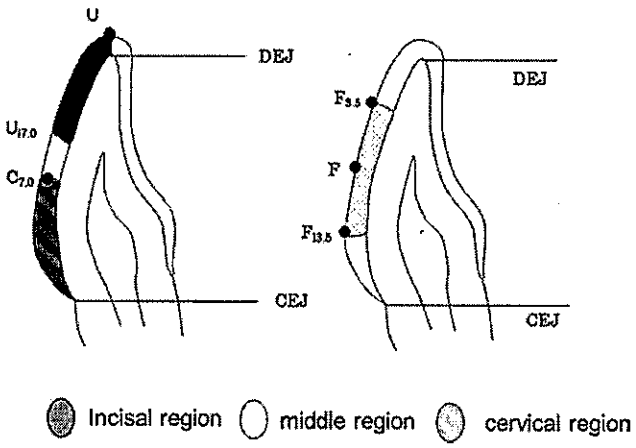

Fig. 5. Schematic showing the labial enamel area according to measurement position. CEJ—cement enamel junction. DEJ—dentin enamel junction.

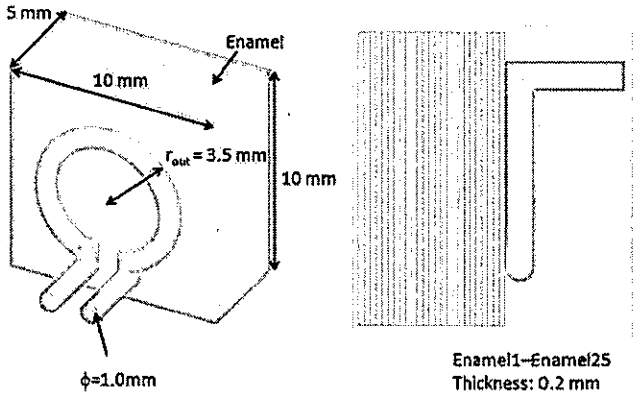

Fig. 6. Finite-element model of a surface coil and enamel. The 3D model of enamel is 5 mm × 10 mm × 10 mm in size and comprises 25 layers, each 0.2 mm in thickness. The diameter of the resonator is 7 mm. The detection loop is made of 1-mm-thick silver wire.

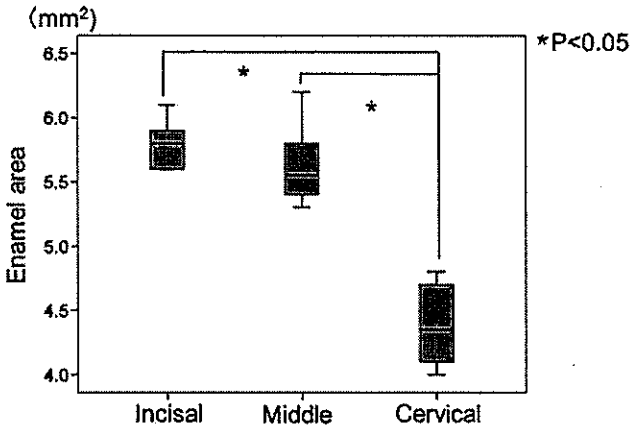

Fig. 7. Enamel area at each position evaluated using micro-CT. All measurements for three locations, i.e., cervical, middle, and incisal regions of tooth, for 10 extracted maxillary central incisors are plotted in this figure. The central mark is the median, the edges of the box are the 25th and 75th percentiles, and the whiskers extend to the most extreme data points. The asterisk indicates a significant difference between the two groups.

calculated at 1.15 GHz using an ANSYS HFSS™ 3D full-wave model microwave field simulator (ver. 13.0.0; Ansys Inc., Canonsburg, PA, USA). A 3D model of the surface loop was used and stacked sheets of enamel for simulations of the RF magnetic fields, as illustrated in Fig. 6. To understand the distribution of the magnetic energy along the depth direction (thickness direction of enamel), the RF magnetic fields around the loop and the magnetic energy in each modeled enamel sheet were calculated. For enamel-model sheets, the dielectric constant ε_r was 7.625, and the dielectric loss tangent tanδ was 0.0656 (Hoshi et al. 1998).

The energy distribution in a sample affects the filling factor and the sensitivity of EPR detection. The energy density of magnetic fields is proportional to the square of magnetic field intensity. The RF magnetic energy in an enamel sheet can be calculated as the integral of the energy density over the enamel sheet. The spatial profile of the magnetic energy in enamel was obtained from the magnetic energy in the enamel sheets of the simulated model.

As illustrated in Fig. 6, the 3D model consisted of a surface loop and 25 sheets of enamel (denoted as Enamel 1–Enamel25) that covered a volume of 5 mm × 10 mm × 10 mm. The thickness of each sheet was 0.2 mm.

The mean diameter of the detection loop was 7 mm, and the loop was made of 1-mm-thick silver wire. Accordingly, the diameter of the detection loop was smaller than the surface of a typical maxillary incisor, which is about 8 × 10.5 mm.

Statistical analysis

Continuous variables are expressed as means ± standard deviations (SDs). Based on the distribution of the continuous variables, they were compared using the Student's *t*-test for two-group analyses or analysis of variance (ANOVA) for three-group analyses. IBM SPSS Statistics ver. 20.0 (IBM Corp., Armonk, NY, USA) was used for all statistical analyses. A p-value <0.05 was considered statistically significant.

RESULTS

Labial enamel thickness and enamel area at each position

The enamel thicknesses at points I, F, C2.0, and C1.5 were 0.84 ± 0.05, 0.73 ± 0.05, 0.45 ± 0.05, and 0.37 ± 0.04 mm, respectively. The labial enamel was more than 0.7 mm thick at both points I and F, whereas the enamel thicknesses at both C2.0 and C1.5 were nearly 50% less than the thicknesses at points I and F. Thus, the enamel was thicker in the incisal region than in the cervical region. Fig. 7 shows the labial enamel area (Fig. 5) at each of the identified measurement positions (cervical, middle, and incisal regions) according to CT measurement.

One-way ANOVA showed that the enamel area was significantly dependent on the measurement position ($p < 0.001$). Multiple comparisons showed that there was a significant difference in enamel area between the incisal and cervical regions ($p < 0.001$) and between the middle and cervical regions ($p < 0.001$). There was no significant difference in enamel area between the incisal and middle regions ($p = 0.26$).

Relationship between enamel area and dose response

The dose responses of the extracted human maxillary central incisors were measured as RelRIS versus the applied dose (Fig. 8). The dose-response curve increased linearly with the radiation dose. The dose response was modeled as αD + β, where D is the applied dose, α is the slope, and β is the intercept. The term "α" denotes the magnitude of the dose response, and "β" denotes the background relative RIS amplitude. Since native signals were too small compared with RIS for a large amount of radiation, it was

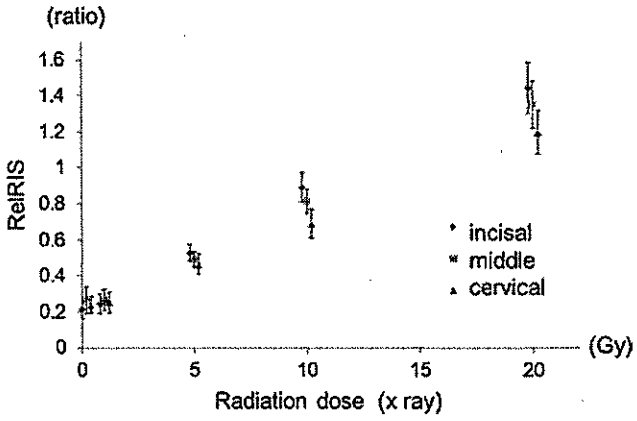

Fig. 8. RelRis response relations for human maxillary incisors irradiated *ex vivo*. Error bar denotes standard deviation (SD).

thought that these signals could be ignored for analyzing relationships between an enamel area of interest and an EPR signal response for unit radiation dose.

The measurements in the incisal region were $\alpha = 0.063 \pm 0.010$ Gy^{-1} and $\beta = 0.211 \pm 0.041$, those in in the middle region were $\alpha = 0.056 \pm 0.079$ Gy^{-1} and $\beta = 0.235 \pm 0.057$, and those in the cervical region were $\alpha = 0.049 \pm 0.079$ Gy^{-1} and $\beta = 0.217 \pm 0.033$. One-way ANOVA showed that α was significantly dependent on the position of the detection loop ($p = 0.005$). Multiple comparisons showed that there was a significant difference in α between the measurements of the incisal and cervical regions of the teeth ($p = 0.003$). However, there was no significant difference in α values between the incisal and middle regions ($p = 0.181$) or between the middle and cervical regions ($p = 0.181$). Moreover, one-way ANOVA showed that β was not significantly dependent on the position of the detection loop ($p = 0.419$).

Fig. 9 shows the relationship between α and the enamel area (Fig. 5) at each point where the detection loop was positioned. The sample size was 10, and the detection loop was positioned at three different sites on the tooth sample (Fig. 2), resulting in a total of 30 points reflecting three measurement regions for each tooth ($\alpha = 0.054$ Gy^{-1}, enamel area = 5.8 mm^2 overlapped).

Linear regression showed that α was significantly dependent on the enamel area ($p < 0.001$). Therefore, α could be modeled using the formula $\alpha = a \times$ (enamel area) $+ b$, where $a = 0.01$ Gy^{-1} m^{-2}, and $b = 0.006$ Gy^{-1}.

It was confirmed that the dosimetric sensitivity, as expressed by α, was dependent on the enamel area.

Simulation

Fig. 10 shows the relationship between the magnetic energy within the enamel at various depths indicated as

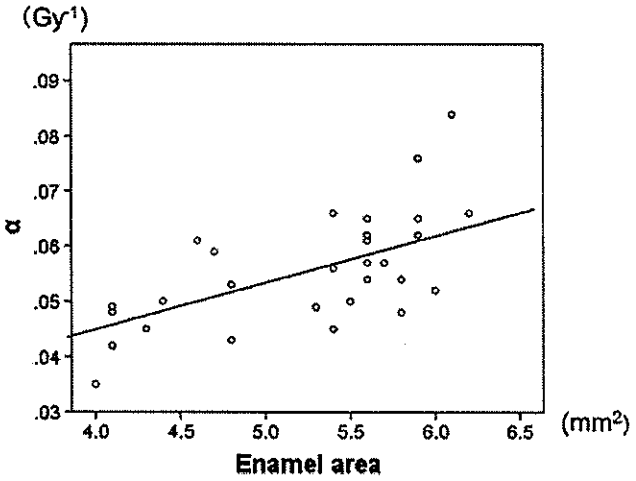

Fig. 9. Relationship between enamel area and α (dosimetry sensitivity). All measurements for three locations—cervical, middle, and incisal regions—of the tooth for 10 extracted maxillary central incisors are plotted in this figure.

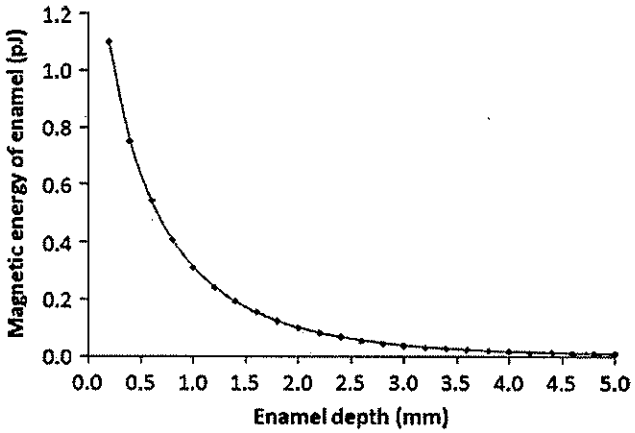

Fig. 10. Relationship between enamel depth and magnetic energy in enamel layer. The magnetic energy in a given volume can be calculated as an integral of the magnetic energy density $(1/2\ \mu_0)\ B_1^2$ over the volume, where B_1 is the RF magnetic flux density and μ_0 is the magnetic permeability of free space. The magnetic permeability of enamel can be treated as the constant μ_0.

layers (Fig. 6) and the distance from the center of each layer to the surface. The results show that the magnetic energy within each of the layers decreased as the depth increased. For the resonator tested, which had a detection loop with an outer diameter of 7.0 mm, the first layer (0–0.2 mm) had energy of about 1.1 pJ, the second layer (0.2–0.4 mm) had energy of about 0.75 pJ, and the sixth layer (1.00–1.2 mm) had energy of about 0.32 pJ. The energy in the sixth layer was 30% of that in the first layer. Although the distribution of the RF magnetic field around the loop is not given in this paper, it can be seen in Fig. 2 of the paper by Pollock et al. (2010). That paper showed the distribution of the RF magnetic field for a circular loop (10 mm in diameter). Although the loop diameter in the paper by Pollock et al. is marginally different from this one, the distribution pattern of the RF magnetic field is comparable.

Fig. 11a shows the relationship between the enamel integrated thickness and the RIS amplitude, and the latter was estimated using a simulation. RIS could be calculated relative to the measured values for magnetic energy in the enamel, which in turn was taken as the integral of the curve shown in Fig. 10, from the surface to the depth of interest. The RIS amplitude expressed in the figure was normalized to that calculated for an enamel thickness of 0.4 mm. This normalized RIS amplitude increased as the enamel thickness increased, reflecting the high amount of RF magnetic energy in the sample.

DISCUSSION

The present study had three main findings. First, the labial enamel thickness and area within the central sagittal plane of the enamel differed depending on the measurement position. Second, the measured relative RIS amplitude

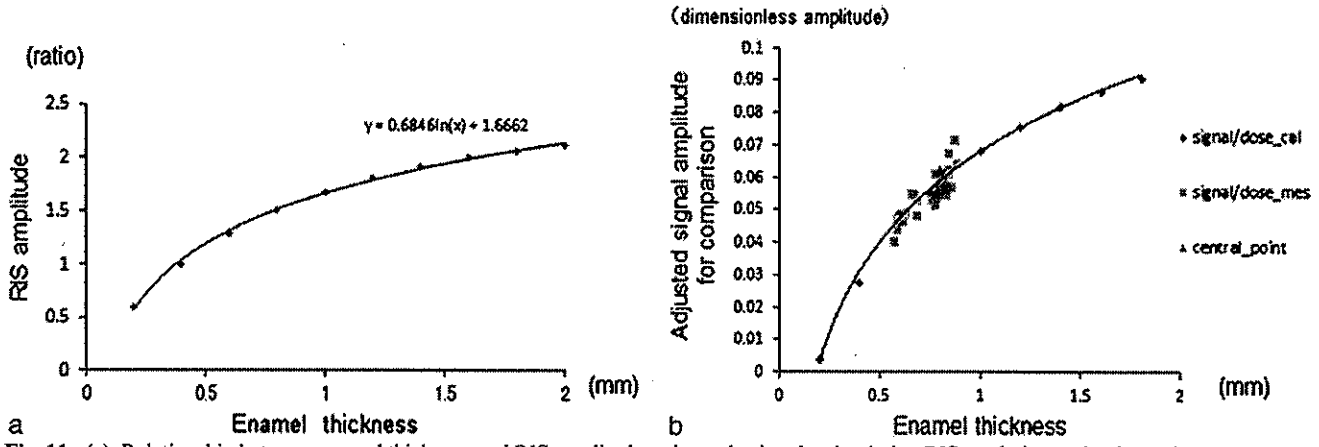

Fig. 11. (a): Relationship between enamel thickness and RIS amplitude estimated using the simulation RIS—relative evaluation at 0.4-mm enamel thickness. Y axis is normalized to 0.4-mm data point; (b): Normalized signal amplitude calculated from the simulation-vs.-measurement signal amplitude. Central point indicates a point that represents the mean enamel thickness and the mean EPR signal amplitude obtained by measurements.

significantly depended on the enamel thickness and measurement position. Third, the incisal and middle regions of the maxillary central incisor were more suited than the cervical region for measurements using a surface-type resonator (7 mm in diameter).

In all types of human teeth, it has been well established that the labial enamel thickness at the incisal region is thicker than that at other regions and that this thickness decreases toward the cervical part of the tooth. Chen et al. (2003) measured the labial enamel thicknesses of maxillary anterior teeth in Chinese subjects (point I = 0.91 ± 0.10 mm, point F = 0.76 ± 0.15 mm, point C2.0 = 0.49 ± 0.09 mm, and point C1.5 = 0.43 ± 0.07 mm). Their results were similar to the present findings in Japanese subjects (point I = 0.84 ± 0.05 mm, point F = 0.73 ± 0.05 mm, point C2.0 = 0.45 ± 0.05 mm, and point C1.5 = 0.37 ± 0.04 mm). A *t*-test showed that there was no significant difference between the data of Chen et al. and the current data (point I: $p = 0.58$; point F: $p = 0.84$; point C2.0: $p = 0.87$; point C1.5: $p = 0.57$). Many reports have shown that teeth are generally larger in male individuals than in female individuals (Garn et al. 1967; Brown and Townsend 1979; Harris and Bailit 1987). The enamel thickness of the maxillary anterior teeth may also differ according to race and gender. Harris and Hicks found that enamel thickness was greater in African American subjects than in European subjects (Harris et al. 2001); however, they also reported that gender-based differences in enamel thickness were low for the mesial-distal side of the maxillary anterior teeth (Harris and Hicks 1998). To date, no studies have compared the enamel thickness in Japanese subjects with that in other races. With aging and other pathological factors, enamel will be gradually ground down by mastication (Gregory-Head and Curtis 1997; Smith et al. 1997). Enamel wears out with a toothbrush, and dentin may be exposed due to wedge-shaped defects in the cervical part. Furthermore, a caries restoration therapy changes enamel thickness.

When attempting to maximize the EPR signal amplitude, the product of the quality factor Q and the filling factor μ of the resonator may be used as an index of relative resonator sensitivity. It is important to design the resonator to maximize μQ, while recognizing that the precision of dose estimation will depend on the amplitude of the noise and its effect on the estimated RIS amplitude. Previous researchers have enhanced the sensitivity and decreased the measured noise levels of resonators, thereby maximizing the accuracy and precision of dose estimation (Haga et al. 2013; Hirata et al. 2000). The surface coil resonator used in this study allowed for remote impedance adjustment with a reasonably high sensitivity; however, the disadvantage of this resonator was the offset of the spectral baseline from interference by magnetic field modulation. The best EPR detection sensitivity was obtained by using a surface coil with an outer diameter of 6 mm and a wire thickness of 1 mm for the surface coil resonator calculations, along with the incisor tooth model described by Sugawara et al. (2014). Smaller surface coils will be more sensitive to different aspects of coil placement, including the angle of placement and position on the tooth. For practical purposes, the coil was made a little larger than the optimal diameter to reduce the influence of coil placement on EPR sensitivity.

The effects of surface-loop positioning in the mouth were previously examined by Pollock et al. (2010), who found that the sensitivity decreased as the loop was moved away from the biting surface of a row of molars. The same study also reported consistency between experimental and simulated results. The separation between the loop and tooth was also considered, but the researchers did not consider the potential effects of variations in enamel thickness. Sensitivity distribution depends on the distribution of RF magnetic fields and the direction of the static magnetic

field. In this study, sensitivity, defined as the slope of the dose response α, varied in relation to the enamel area at the measurement position. These simulation data showed that the amount of magnetic energy within the enamel was related to the enamel thickness at the measurement position. As the enamel thickness increased, the energy in subsequent layers reduced exponentially. However, as the enamel thickness increased, the energy within the whole volume of enamel, the filling factor μ, and the EPR signal amplitude increased.

The labial enamel thickness at the defined incisal region was approximately 0.8 mm, whereas the thickness in the cervical region was approximately 0.4 mm. The current simulation results predicted that the EPR signal strength would fall by 1.5 times if the enamel thickness falls from 0.8 mm to 0.4 mm.

The simulated signal amplitudes for each thickness of enamel in a maxillary central incisor were compared with the measured signal amplitudes by using a least-squares method (Fig. 11b). The normalized signal amplitude increased at the same rate in both the simulation and the measurement.

In vivo L-band EPR spectrometric measurements at the cervical region will not be accurate in the presence of excess saliva, gum tissue, or very thin enamel. With respect to enamel thickness, it is desirable to perform in vivo L-band EPR spectrometric measurements near the incisal region for all types of teeth.

Sunlight can appreciably contribute to the measured dose in the tooth enamel of the front teeth. The contribution has been reported to be as large as that by 200 mGy (Sholom et al. 2010). However, according to the EPR tooth dosimetry results, the relative contribution of signals due to UV light exposure to tooth enamel for triage decisions is expected to be small. Indeed, a previous study suggested that natural UV exposure does not cause detectable signals when using L-band EPR spectrometric measurements in vivo (Miyake et al. 2016).

If one uses a small surface loop for EPR measurements, the detected volume of enamel becomes small. Also, the thickness of enamel in incisors is not constant in terms of the placement of the loop on the subject incisor. Therefore, the detected volume of enamel depends on the position of the surface loop, as well as the shape and the size of the loop. Resonators with detection loops designed for measurement over the incisal region of teeth should be further developed to increase their sensitivity. When conducting in vivo measurements, it is necessary to consider the impact of surrounding glossy tissues, such as the gingiva, to simultaneously minimize the impact of associated dielectric losses. If the diameter of the surface loop is very small in comparison to a teeth sample, the measured volume of the teeth depends on the thickness of enamel and the diameter of the surface loop. Such a circumstance is similar to that with the use of the pinhole of a cavity resonator at X-band EPR spectroscopy reported by Ikeya and his colleagues (Ishii and Ikeya 1990; Hochi et al. 1993).

In this study, the sample size was small, partly owing to the difficulty associated with the collection of intact human maxillary incisors. Therefore, in addition to extending the measurements to a larger sample, the authors plan to measure RIS differences related to age, race, enamel maturity, and deciduous teeth.

CONCLUSION

The amplitude of the radiation-induced EPR signal is significantly dependent on the location of the EPR detection loop over the maxillary central incisor surface, largely because of the thickness of the underlying enamel. The incisal and middle regions of the incisor are more suitable than the cervical region for measurements using a surface-type resonator.

Acknowledgments—This work was supported by Japan Society for the Promotion of Science KAKEN (grant number #26462841) and Japan Industrial Disease Clinical Research Grant (#150803-02).

REFERENCES

Brown T, Townsend G. Sex determination by single and multiple tooth measurements. Australian Institute of Aboriginal Studies; 1979.

Chen K, Lin W, Shin S, Terashita M. Labial enamel thickness of Chinese for porcelain laminate veneer. J Dent Res 82: 400–400; 2003.

Desrosiers M, Schauer DA. Electron paramagnetic resonance (epr) biodosimetry. Nucl Instrum Methods Phys Res B 184: 219–228; 2001.

Feher G. Sensitivity considerations in microwave paramagnetic resonance absorption techniques. Bell System Technical J 36: 449–484; 1957.

Flood AB, Boyle HK, Du G, Demidenko E, Nicolalde RJ, Williams BB, Swartz HM. Advances in a framework to compare biodosimetry methods for triage in large-scale radiation events. Radiat Protect Dosim 159:77–86; 2014.

Flood AB, Nicolalde RJ, Demidenko E, Williams BB, Shapiro A, Wiley AL Jr, Swartz HM. A framework for comparative evaluation of dosimetric methods to triage a large population following a radiological event. Radiat Meas 46:916–922; 2011.

Garn SM, Lewis AB, Swindler DR, Kerewsky RS. Genetic control of sexual dimorphism in tooth size. J Dent Res 46: 963–972; 1967.

Gregory-Head B, Curtis DA. Erosion caused by gastroesophageal reflux: diagnostic considerations. J Prosthodontics 6: 278–285; 1997.

Haga T, Hirata H, Lesniewski P, Rychert KM, Williams BB, Flood AB, Swartz HM. L-band surface-coil resonator with voltage-control impedance-matching for EPR tooth dosimetry. Concepts Magn Reson Part B Magn Reson Eng 43:32–40; 2013.

Harris E, Bailit H. Odontometric comparisons among Solomon islanders and other oceanic peoples. In: The Solomon Islands Project: a long-term study of health, human biology, and culture change. Oxford: Clarendon Press; 215–264; 1987.

Harris EF, Hicks JD. A radiographic assessment of enamel thickness in human maxillary incisors. Arch Oral Biol 43: 825–831; 1998.

Harris EF, Hicks JD, Barcroft BD. Tissue contributions to sex and race: differences in tooth crown size of deciduous molars. Am J Phys Anthropol 115:223–237; 2001.

Hirata H, He G, Deng Y, Salikhov I, Petryakov S, Zweier JL. A loop resonator for slice-selective in vivo EPR imaging in rats. J Magn Reson 190:124–134; 2008.

Hirata H, Walczak T, Swartz HM. Electronically tunable surface-coil-type resonator for l-band epr spectroscopy. J Magn Reson 142:159–167; 2000.

Hochi A, Furusawa M, Ikeya M. Applications of microwave scanning ESR microscope: human tooth with metal. Appl Radiat Isot 44:401–405; 1993.

Hoshi N, Nikawa Y, Kawai K, Ebisu S. Application of microwaves and millimeter waves for the characterization of teeth for dental diagnosis and treatment. IEEE Trans Microwave Theory Techniques 46:834–838; 1998.

Ikeya M, Miki T, Kai A, Hoshi M. ESR dosimetry of a-bomb radiation using tooth enamel and granite rocks. Radiat Protect Dosim 17:181–184; 1986.

Ikeya M, Miyajima J, Okajima S. ESR dosimetry for atomic bomb survivors using shell buttons and tooth enamel. Jpn J Appl Phys 23:L697–L699; 1984.

Ishii H, Ikeya M. An electron spin resonance system for in-vivo human tooth dosimetry. Japanese J Applied Phys 29: 871; 1990.

Iwasaki A, Walczak T, Grinberg O, Swartz HM. Differentiation of the observed low frequency (1200 mhz) EPR signals in whole human teeth. Appl Radiat Isot 62:133–139; 2005.

Miyake M, Liu KJ, Walczak TM, Swartz HM. In vivo EPR dosimetry of accidental exposures to radiation: experimental results indicating the feasibility of practical use in human subjects. Appl Radiat Isot 52:1031–1038; 2000.

Miyake M, Nakai Y, Yamaguchi I, Hirata H, Kunugita N, Williams BB, Swartz HM. In-vivo radiation dosimetry using portable l band EPR: on-site measurement of volunteers in Fukushima prefecture. Japan. Radiat Protect Dosim 172:248–253; 2016.

Pollock JD, Williams BB, Sidabras JW, Grinberg O, Salikhov I, Lesniewski P, Kmiec M, Swartz HM. Surface loop resonator design for in vivo EPR tooth dosimetry using finite element analysis. Health Phys 98:339–344; 2010.

Sholom S, Desrosiers M, Chumak V, Luckyanov N, Simon S, Bouville A. UV effects in tooth enamel and their possible application in EPR dosimetry with front teeth. Health Phys 98: 360; 2010.

Smith BG, Bartlett DW, Robb ND. The prevalence, etiology and management of tooth wear in the United Kingdom. J Prosthetic Dent 78:367–372; 1997.

Sugawara H, Hirata H, Petryakov S, Lesniewski P, Williams B, Flood A, Swartz H. Design and evaluation of a 1.1-ghz surface coil resonator for electron paramagnetic resonance-based tooth dosimetry. IEEE Trans Biomed Eng 61:1894–1901; 2014.

Swartz HM, Flood AB, Gougelet RM, Rea ME, Nicolalde RJ, Williams BB. A critical assessment of biodosimetry methods for large-scale incidents. Health Phys 98:95–108; 2010.

Swartz HM, Flood AB, Williams BB, Dong R, Swarts SG, He X, Grinberg O, Sidabras J, Demidenko E, Gui J, Gladstone DJ, Jarvis LA, Kmiec MM, Kobayashi K, Lesniewski PN, Marsh SD, Matthews TP, Nicolalde RJ, Pennington PM, Raynolds T, Salikhov I, Wilcox DE, Zaki BI. Electron paramagnetic resonance dosimetry for a large-scale radiation incident. Health Phys 103:255–267; 2012.

Swartz HM, Iwasaki A, Walczak T, Demidenko E, Salikov I, Lesniewski P, Starewicz P, Schauer D, Romanyukha A. Measurements of clinically significant doses of ionizing radiation using non-invasive in vivo EPR spectroscopy of teeth in situ. Appl Radiat Isot 62:293–299; 2005.

Swartz HM, Williams BB, Zaki BI, Hartford AC, Jarvis LA, Chen EY, Comi RJ, Ernstoff MS, Hou H, Khan N, Swarts SG, Flood AB, Kuppusamy P. Clinical EPR: unique opportunities and some challenges. Acad Radiol 21:197–206; 2014.

Williams BB, Dong R, Flood AB, Grinberg O, Kmiec M, Lesniewski PN, Matthews TP, Nicolalde RJ, Raynolds T, Salikhov IK, Swartz HM. A deployable in vivo EPR tooth dosimeter for triage after a radiation event involving large populations. Radiat Meas 46:772–777; 2011a.

Williams BB, Dong R, Kmiec M, Burke G, Demidenko E, Gladstone D, Nicolalde RJ, Sucheta A, Lesniewski P, Swartz HM. Development of in vivo tooth EPR for individual radiation dose estimation and screening. Health Phys 98:327–338; 2010.

Williams BB, Dong R, Nicolalde RJ, Matthews TP, Gladstone DJ, Demidenko E, Zaki BI, Salikhov IK, Lesniewski PN, Swartz HM. Physically-based biodosimetry using in vivo EPR of teeth in patients undergoing total body irradiation. Int J Radiat Biol 87:766–775; 2011b.

Williams BB, Flood AB, Salikhov I, Kobayashi K, Dong R, Rychert K, Du G, Schreiber W, Swartz HM. In vivo EPR tooth dosimetry for triage after a radiation event involving large populations. Radiat Environ Biophys 53:335–346; 2014.